Revisiting Spurious-Free Dynamic Range of Communication Receivers

Jongrit Lerdworatawee, *Student Member, IEEE,* and Won Namgoong, *Member, IEEE*

***Abstract*—The spurious free dynamic range (SFDR) is commonly used as a measure of dynamic range for the radio frequency and microwave front-end receivers. Although well defined in narrow-band systems, the definition becomes less clear in wide-band systems, when the nonlinearity is memoryless and the the noise figure is frequency dependent. To generalize the SFDR to wide-band systems, a meaningful physical interpretation of the conventional two-tone test is first developed. Based on this interpretation, the upper bound of the wide-band SFDR is obtained by applying a multitone test, while the lower bound is computed using the effective noise figure. The multitone test in both the memoryless and memory nonlinear Volterra systems is considered. A practical measurement technique to characterize the Volterra kernel is also provided. A realistic example based on a low noise amplifier shows a significant difference between the conventional and wide-band SFDR values. In this example, our results suggest that the use of two tones widely separated in frequency to model the interferers provides sufficiently accurate results compared to a multitone approximation.**

***Index Terms*—Circuit theory, distortion analysis, dynamic range, intermodulation product, noise figure, Volterra series, wideband communications circuit.**

I. Introduction

In radio-frequency (RF) and microwave front-end receivers, the spurious-free dynamic range (SFDR) is commonly used to determine the input power range in which the received signal can be detected in the presence of noise and amplified without nonlinear interference [1], [2]. The lower bound of the SFDR is set by the input-referred noise floor, which is determined by the receiver noise figure (NF). The upper bound is defined as the interferer power level at which an undesirable intermodulation product equals the noise power. This undesirable product is the third-order intermodulation product term (IM_3), which is typically the dominant source of nonlinear interference. As a result, we subsequently consider the third-order nonlinearity only when determining the upper bound of the SFDR. The IM_3 is incorporated into the SFDR expression by determining the input-referred third-order intercept point (IIP3), which can be readily obtained experimentally using the two-tone test.

The underlying assumption when computing the SFDR is that the NF is constant and the nonlinear system is memoryless. Since this assumption is valid only in narrow-band systems, the SFDR is not well defined in wide-band systems. In this paper, a modified definition of SFDR is proposed to generalize the conventional SFDR to wide-band systems. In this definition, the NF metric used to determine the lower bound is the effective NF proposed in [3]. Defined as the weighted harmonic mean of the measured spot NF across the frequency band of interest, the effective NF represents the loss in the achievable performance after the digital signal processing. To determine the upper bound, a multitone test based on a meaningful physical interpretation of the conventional two-tone test is proposed. In this test, the input tones are viewed as approximating the input interference signal spectrum. The upper bound then corresponds to the maximum nonlinear interference in the signal band of interest when all third-order nonlinear products (including IM_3) are considered.

The organization of this paper is as follows. In Section II, the Volterra series expansion which is used to characterize the general nonlinear system [4]–[7] is reviewed. Section III presents a modified definition of SFDR so that it can be extended to wide-band systems. The SFDR of a memoryless nonlinear system is discussed in Section IV. The SFDR of a general Volterra system is described in Section V, including numerical results. Conclusions are drawn in Section VI.

II. Review of the Volterra Series Expansion

Consider a weakly nonlinear system with input $x(t)$ and output $y(t)$. According to the Volterra theory [5]–[7], the nonlinear system can be modeled as an infinite sum of the linear response (first order) $y_1(t)$ and the higher order nonlinear response $y_k(t)$ (for $k > 1$) as shown in Fig. 1. The total response at the output can then be written as

$$\begin{aligned} y(t) &= \sum_{k=1}^{\infty} y_k(t) \\ &= \sum_{k=1}^{\infty} \int \cdots \int h_k(\tau_1, \ldots, \tau_k) \left(\prod_{i=1}^{k} x(t-\tau_i) \right) \\ &\quad \times d\tau_1, \ldots, d\tau_k \end{aligned} \tag{1}$$

where $h_k(\tau_1, \ldots, \tau_k)$ is the Volterra kernel of the nth-order Volterra system.

Suppose that the input of the nonlinear system consists of Q equally-powered sinusoidal signals, i.e., [8], [9]

$$\begin{aligned} x(t) &= \sum_{q=1}^{Q} A \cos(2\pi f_q t + \theta_q) \\ &= \frac{1}{2} \sum_{\substack{q=-Q \\ q \neq 0}}^{Q} A \exp\{j(2\pi f_q t + \theta_q)\} \end{aligned} \tag{2}$$

Manuscript received December 24, 2004; revised June 30, 2005 and September 17, 2005. This work was supported in part by the Army Research Office under Contract DAAD19-01–1–0477 and by the National Science Foundation under Grant ECS-0134629. This paper was recommended by Associate Editor G. Palumbo.

The authors are with the Department of Electrical Engineering, University of Southern California (e-mail: lerdwora@usc.edu; namgoong@usc.edu).

Digital Object Identifier 10.1109/TCSI.2005.861891

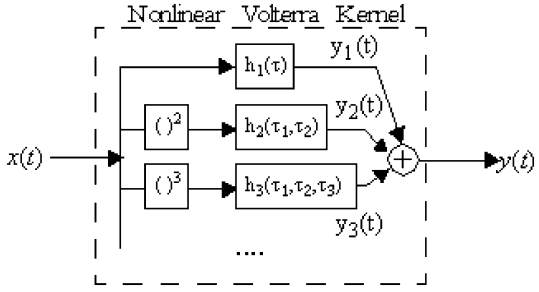

Fig. 1. General memory weakly nonlinear system.

where A denotes the magnitude, and f_q and θ_q are the frequencies and phases, respectively, of the qth input tone, for $q \in \{1, \ldots, Q\}$. Note that the frequency with the negative index is defined as the negative frequency, e.g., $f_{-q} = -f_q$.

Substituting (2) into (1), the output of the kth-order Volterra system is given by [10], [11]

$$y_k(t) = \left(\frac{A}{2}\right)^k \sum_{\substack{q_1=-Q \\ q_1\neq 0}}^{Q} \cdots \sum_{\substack{q_k=-Q \\ q_k\neq 0}}^{Q} H_k(f_{q_1}, \ldots, f_{q_k}) \times \exp\left\{ j \sum_{i=1}^{k} (2\pi f_{q_i} t + \theta_{q_i}) \right\} \quad (3)$$

where $H_k(f_{q_1}, \ldots, f_{q_k}) = |H_k(f_{q_1}, \ldots, f_{q_k})| \exp\{\theta_k(f_{q_1}, \ldots, f_{q_k})\}$ is the k-dimensional Fourier transform of $h_k(\tau_1, \ldots, \tau_k)$. Since the Volterra kernels are generally real in time domain in practice, their frequency domain representations are conjugate symmetric.

A. Classifying the Nonlinearity Products

Throughout this paper, we assume that the nonlinear interference of the receiving system is dominated by the third-order nonlinearity product (NL_3). The second-order nonlinear interference generate out of band frequency components, and therefore, they are ignored. Although the subsequent analysis can be generalized to include higher order distortions, they are assumed to be negligible for simplicity.

Denoting f_q (or f_{-q}) as the positive (or negative) frequency of the qth input tone and a nonnegative integer m_q as the number of times that f_q appears in the Volterra kernel, the frequency of the NL_3 term can be written in terms of the frequency mixes (i.e., the sum of f_q weighted by m_q) by [7]

$$f_{\mathrm{NL3}} = \sum_{\substack{q=-Q \\ q\neq 0}}^{Q} m_q f_q \quad (4)$$

where the weight m_q is subject to the following constraint:

$$\sum_{\substack{q=-Q \\ q\neq 0}}^{Q} m_q = 3. \quad (5)$$

According to (4) and (5), the frequency mix which generates the inband NL_3 consists of either two or three separate frequencies, where the positive and negative frequencies are counted separately. For both cases, the frequency mix that generates a positive inband NL_3 is always generated from two positive frequencies (which we refer to as f_a and f_b) and one negative frequency (i.e., f_{-c}) for $a, b, c \in \{1, \ldots, Q\}$. When NL_3 is generated from two separate frequencies, which occurs when $a = b$, we refer to it as the two-toned NL_3. Similarly, when $a \neq b$, the resulting NL_3 is referred to as the three-toned NL_3. A distinction between the two-toned and the three-toned NL_3 are made because of the difference in the magnitude of the resulting NL_3 tone as described shortly. In both cases, the resulting NL_3 tone frequency becomes the direct sum of f_a, f_b and $-f_c$, i.e.,

$$f_{\mathrm{NL3}} = f_a + f_b - f_c. \quad (6)$$

As an example of possible frequency mixes that generate NL_3, consider a three-tone test where the positive frequencies are denoted as f_1, f_2, and f_3. Examples of the two-toned NL_3 are $2f_1 - f_1$, $2f_1 - f_2$ and $2f_1 - f_3$, where $(a, b, -c)$ are (1, 1, -1), (1, 1, -2) and (1, 1, -3), respectively. The first frequency mix (where $a = b = c$) results in gain compression/expansion [12]; while the last two are typically referred to as the third-order intermodulation product, which we denote as IM_3 [12]. Examples of the three-toned NL_3 are $f_1 + f_2 - f_1$, $f_1 + f_3 - f_2$ and $f_1 + f_2 - f_3$, where $(a, b, -c)$ are (1, 2, -1), (1, 3, -2) and (1, 2, -3), respectively. The first frequency mix (i.e., $a = c$) causes gain desensitization [12]; while the last two are the frequency mixes of three different frequencies, which we subsequently refer to as three-tone frequency mix. In this paper, we consider all third-order nonlinear distortions, not just the IM_3 terms, when determining the SFDR.

B. Expressing the Nonlinear Products' Power

Based on (3), the amplitude of the NL_3 tone at f_{NL3} is

$$|Y_3(f_{\mathrm{NL3}})| = \frac{3}{4} \left| \sum_{(a,b,c)\in S(f_{\mathrm{NL3}})} \gamma_{ab} H_3(f_a, f_b, -f_c) \times \exp[j(\theta_a + \theta_b - \theta_c)] \right| A^3 \quad (7)$$

where f_a, f_b and f_c are given according to (6) and S_{NL3} denotes the set of all possible combinations of the indexes (a, b, c) at which (6) is satisfied for a given f_{NL3}, i.e.,

$$S(f_{\mathrm{NL3}}) = \{(a, b, c) |\, f_a + f_b - f_c = f_{\mathrm{NL3}}, \; 1 \le a, b, c \le Q\} \quad (8)$$

and

$$\gamma_{ab} = \begin{cases} 1, & a = b \\ 2, & a \neq b \end{cases} \quad (9)$$

is used to differentiate between the two-toned and three-toned NL_3 [7]. Using (7), the corresponding power of the NL_3 at f_{NL3} is

$$\begin{aligned} P_{\mathrm{NL3}}^{(Q)}(f_{\mathrm{NL3}}) &= \frac{E[|Y_3(f_{\mathrm{NL3}})|^2]}{2R_s} \\ &= \left(\frac{9A^6}{32R_s}\right) \times E\left\{ \left| \sum_{(a,b,c)\in S(f_{\mathrm{NL3}})} \gamma_{ab} H_3(f_a, f_b, -f_c) \times \exp[j(\theta_a + \theta_b - \theta_c)] \right|^2 \right\} \\ &= \left(\frac{9A^6}{32R_s}\right) \sum_{(a,b,c)\in S(f_{\mathrm{NL3}})} \gamma_{ab}^2 |H_3(f_a, f_b, -f_c)|^2 \end{aligned} \quad (10)$$

where R_S is the source resistance (typically 50 Ω) and the phases of the equally spaced multiple sinusoidal tones applied to the input of a memoryless system are assumed to be independent random variables that are uniformly distributed from 0 to 2π.

A common measure of the degree of nonlinearity is the intercept point, which occurs in the two-tone test when the input-referred fundamental and IM_3 powers are equal. A similar measure of nonlinearity can be obtained when Q tones are applied by defining the Q-tone IIP3 $P_{\mathrm{IIP3}}^{(Q)}(f_{\mathrm{NL3}})$ as the input power of a single tone that equals the input-referred NL_3 power at f_{NL3}. Mathematically, $P_{\mathrm{IIP3}}^{(Q)}(f_{\mathrm{NL3}})$ can be determined by equating (7) to the fundamental magnitude (i.e., $|H_1(f_{\mathrm{NL3}})|A$) and solving the resulting equation for A, i.e.,

$$P_{\mathrm{IIP3}}^{(Q)}(f_{\mathrm{NL3}}) = \frac{2}{3R_s}\frac{|H_1(f_{\mathrm{NL3}})|}{\sqrt{\sum_{(a,b,c)\in S(f_{\mathrm{NL3}})}\gamma_{ab}^2|H_3(f_a,f_b,-f_c)|^2}}. \tag{11}$$

Note that when $Q = 2$ and only the IM_3 terms are considered, (11) reduces to the conventional IIP3, i.e., $P_{\mathrm{IIP3}} = (2/3R_S)|H_1/H_3|$ (where $H_k(f_{q_1},\ldots,f_{q_k}) = H_k$ for any k). $P_{\mathrm{IIP3}}^{(Q)}(f_{\mathrm{NL3}})$ is subsequently used to determine the upperbound of the wide-band SFDR definition.

III. Spurious Free Dynamic Range

A. Reviewing the Conventional SFDR Definition

The SFDR is the input signal power range in which the received signal can be detected in the presence of noise and amplified without nonlinear distortion [1], [2]. The upper bound (P_U) of the conventional SFDR is defined as the input signal power at which the IM_3 power equals the noise power at the output and its lower bound is simply the input signal power that results in a signal-to-noise ratio (SNR) of 0 dB. The lower bound (P_L) can be obtained by computing the input referred noise power N_O, which is the product of the thermal noise power spectral density (kT), the bandwidth of interest (B), and the NF (or simply F), i.e., $N_O = kTFB$.

The upper bound of the conventional SFDR is determined by applying two sinusoidal signals with equal power that are closely spaced in frequency. Assuming the two frequencies are at f_1 and f_2, the linear output power (e.g., at f_1) and the IM_3 product output power (e.g., at $2f_1 - f_2$) are plotted against the power of the input tone P_{in} $(= A^2/2R_S$, where R_S is 50 Ω and A is the tone amplitude). As shown in Fig. 2, they are illustrated by lines 1 and 2, respectively. Using the input referred noise power N_O and the IIP3 (i.e., $P_{\mathrm{IIP3}} = (2/3R_S)\,|H_1/H_3|$), which occurs at the intercept of lines 1 and 2, the upper bound and lower bound of the SFDR can be readily shown to be $P_U = (P_{\mathrm{IIP3}})^{2/3}(N_O)^{1/3}$ and $P_L = N_O$, respectively. Using P_U and P_L, the SFDR (as expressed in decibels) can is given by

$$\begin{aligned}\mathrm{SFDR} &= 10\log_{10}\left(\frac{P_U}{P_L}\right) = 10\log_{10}\left(\frac{P_{\mathrm{IIP3}}}{N_O}\right)^{2/3}\\ &= 10\log_{10}\left(\frac{2}{3kTFBR_S}\left|\frac{H_1}{H_3}\right|\right)^{2/3}.\end{aligned} \tag{12}$$

The underlying assumption when computing the SFDR is that the nonlinear system is memoryless and the NF is constant in the frequency bandwidth of interest B. In wide-band systems, both of the assumptions are not necessarily valid. As a result, the conventional SFDR definition is generalized as described in subsequent sections so that it remains meaningful in wide-band systems.

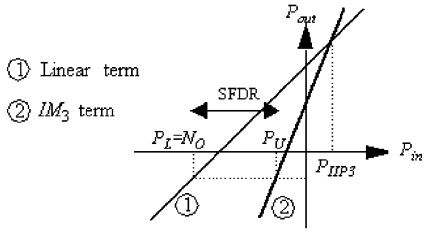

Fig. 2. Computing SFDR using the power tranfer characteristic plot.

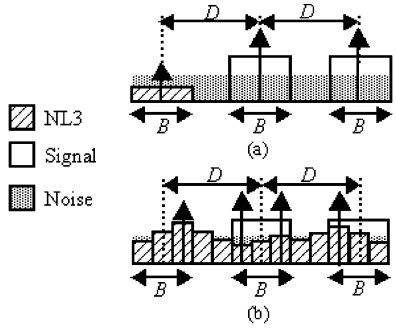

Fig. 3. 2-tone and Q-tone approximation.

B. Multitone Test

The modified definition of SFDR is based on a meaningful physical interpretation of the conventional two-tone test. As shown in Fig. 3(a), the two input tones are viewed as approximating the signal spectrum of two interferers, each of which consists of a constant power-spectral density (PSD) of magnitude S_S and bandwidth B and is separated by D. Each tone with power $P_S = S_S B$ then models the spectrum of one of the interferers. When viewed from this physical perspective, an improved approximation of S_S is possible by employing $Q(>2)$ tones instead of two tones as in the conventional two-tone test. In this multitone test (or Q-tone test), $Q/2$ tones that are equally spaced with a frequency spacing of $\Delta f(= 2B/Q)$ Hz are each used to approximate one of the interferer signal spectrum. In addition, each of the Q input tones are assumed to have equal power $P_{\mathrm{in}}(= 2P_S/Q)$ and independent phase. When multiple tones are applied, not only IM_3 but all other NL_3 products must be considered. An example is illustrated in Fig. 3(b), where the input referred NL_3 product at a particular frequency (as illustrated by the short arrow) is generated by the frequency mix of three input tones (as illustrated by the long arrows).

C. Defining the Wide-band SFDR

Using the Q-tone test, the upper bound of the wide-band SFDR is defined as the minimum P_S at which the maximum NL_3 power-to-noise power ratio (NNR) in the frequency band of interest, or Ω_B, equals to one (or 0 dB) as Q goes to infinity (or equivalently, Δf goes to zero). To compute P_U, the first step

is to search over Ω_B for f_{NL3} corresponding to the maximum NNR. Note that this f_{NL3}, which we denote as f^*, is the same regardless of P_S as can be readily observed from (10). The search for f^* can be mathematically written as

$$f^* = \arg\max_{f_{\mathrm{NL3}}\in\Omega_B}\left\{\frac{P_{\mathrm{NL3}}^{(Q)}(f_{\mathrm{NL3}})}{N_O^{(Q)}(f_{\mathrm{NL3}})|H_1(f_{\mathrm{NL3}})|^2}\right\} \tag{13a}$$

$$= \arg\max_{f_{\mathrm{NL3}}\in\Omega_B}\left\{\left(P_{\mathrm{IIP3}}^{(Q)}(f_{\mathrm{NL3}})\right)^2 N_O^{(Q)}(f_{\mathrm{NL3}})\right\} \tag{13b}$$

where $N_O^{(Q)}(f_{\mathrm{NL3}}) = kTF(f_{\mathrm{NL3}})\Delta f$ is the input noise power in the subband with the bandwidth of Δf and the center at f_{NL3}. Note that, to obtain (13b), we substitute (10) into (13a) and then compare the result with (11). Once f^* is determined, the upperbound is then computed by solving for P_S at which NNR at f^* is equal to 0 dB. The upperbound of SFDR can be shown to be

$$P_U = \left[P_{\mathrm{IIP3}}^{(Q)}(f^*)\right]^{2/3}\left[N_O^{(Q)}(f^*)\right]^{1/3}\left(\frac{Q}{2}\right) \tag{14}$$

where the multiplication by $Q/2$ is necessary as P_U of the wide-band SFDR is defined in terms of P_S instead of P_{in} as in the conventional SFDR.

The lower bound (P_L) of the wide-band SFDR is based on the equivalent noise power in the frequency band of interest. A potential difficulty of computing P_L is that its spot NF varies with frequency, resulting in a nonflat noise spectrum. As described in [3], the equivalent NF (subsequently referred to as F_{eff}) is the harmonic mean of the spot NF $F(f)$ within the bandwidth of B. Consequently, the equivalent noise power N_{eff} is F_{eff} times kTB, and the lower bound is then simply

$$P_L = N_{\mathrm{eff}} = kTBF_{\mathrm{eff}}. \tag{15}$$

Note that the lower bound is the same as in the conventional SFDR when the spot NF is constant in the frequency band of interest, since F_{eff} becomes the spot NF.

Having defined the upper and lower bounds in (14) and (15), the wide-band SFDR can be computed by taking the limit as Q goes to infinity (or equivalently, Δf goes to zero), i.e., we obtain (16), shown at the bottom of the page.

IV. Memoryless Multi-Tone Test

In this section, the wide-band SFDR definition is used to determine the SFDR of a nonlinear system that is memoryless and has constant NF in the frequency band of interest. Under these assumptions, the wide-band SFDR in (16) can be simplified as

$$\mathrm{SFDR} = \lim_{Q\to\infty} 10\log_{10}\left[\left(\frac{2}{3kTFBR_S}\left|\frac{H_1}{H_3}\right|\right)^{2/3} \times \min_{f_{\mathrm{NL3}}\in\Omega_B}\left(\frac{\left(\frac{Q}{2}\right)^2}{\sum_{(a,b,c)\in S(f_{\mathrm{NL3}})}\gamma_{ab}^2}\right)^{1/3}\right] \tag{17}$$

which reduces to the conventional SFDR when $Q = 2$ (see (12)). According to (17), the computation of SFDR entails searching for f_{NL3} to maximize the summation in the denominator of the second bracket, which requires enumerating all NL_3 products that are generated at f_{NL3}. In this section, the enumeration process is first described before comparing the wide-band and conventional SFDR in a memoryless system.

A. Enumerating the NL_3 Terms

Given Q input tones, all the NL_3 products that are generated at f_{NL3} are enumerated. For clarity of discussion, the enumeration procedure is described using an example of equally spaced four-tone test. Here, the input frequencies are denoted as f_0, f_1, f_2 and f_3 and the difference between two frequencies is a multiple of Δf. To enumerate all possible NL_3 combinations that generate f_{NL3}, we sequentially vary f_a in (6) from f_0 to f_3. According to (6), the frequency mix can be written as

$$f_{\mathrm{NL3}} = \left\{\begin{matrix} f_0 \\ f_1 \\ f_2 \\ f_3 \end{matrix}\right\} + (f_b - f_c) \tag{18}$$

where the rows in the bracket on the right-hand side of (18) corresponds to the different positive frequencies (f_a) in the frequency mix. For the case of $f_{\mathrm{NL3}} = f_2$, for example, the remaining positive (f_b) and negative (f_c) frequencies are selected such that their difference satisfy the following equations:

$$f_b - f_c = f_2 - \left\{\begin{matrix} f_0 \\ f_1 \\ f_2 \\ f_3 \end{matrix}\right\} = \left\{\begin{matrix} 2 \\ 1 \\ 0 \\ -1 \end{matrix}\right\}\Delta f \tag{19}$$

which is obtained according to (18).

In each row of (19), multiple choices of f_b and f_c that generate $f_{\mathrm{NL3}} = f_2$ are possible. The enumeration of f_a, f_b and f_c can be better illustrated using the arrow diagram as shown in Fig. 4, where the arrows in each row correspond to the same f_a values and the direction of the arrows are from the column f_c to f_b. For example, arrows 1 and 2 at the bottom row of Fig. 4 correspond to frequency mix of $f_0 + (f_2 - f_0)$ and $f_0 + (f_3 - f_1)$, respectively.

When enumerating all frequency mixes that generate NL_3 at f_{NL3}, it is important to distinguish between contributions from the two-toned NL_3 (when $a = b$) and three-toned NL_3 (when $a \neq b$) as their values of γ are different. Using the arrow diagram, a frequency mix of the two-toned NL_3 occurs when the frequency to which the arrow is pointing is the same as the row in which it belongs. In our example, the two-toned NL_3 are arrows 0 and 3, which represent the gain expansion/compression and IM_3 terms, respectively. By removing the arrows corresponding to the two-toned NL_3, the remaining arrows are the

$$\mathrm{SFDR} = \lim_{Q\to\infty} 10\log_{10}\left(\frac{P_U}{P_L}\right) = \lim_{Q\to\infty} 10\log_{10}\left[\left(\frac{2}{3kTF_{\mathrm{eff}}BR_S}\right)^{2/3}\min_{f_{\mathrm{NL3}}\in\Omega_B}\left(\frac{\left(\frac{Q}{2}\right)^2 F(f_{\mathrm{NL3}})|H_1(f_{\mathrm{NL3}})|^2}{\sum_{(a,b,c)\in S(f_{\mathrm{NL3}})} F_{\mathrm{eff}}\gamma_{ab}^2|H_3(f_a,f_b,-f_c)|^2}\right)^{1/3}\right] \tag{16}$$

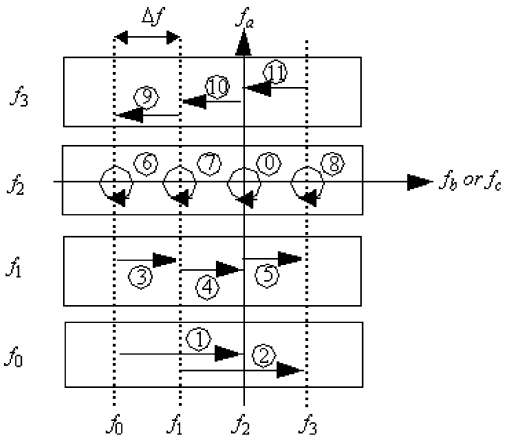

Fig. 4. Equally spaced 4 tone test.

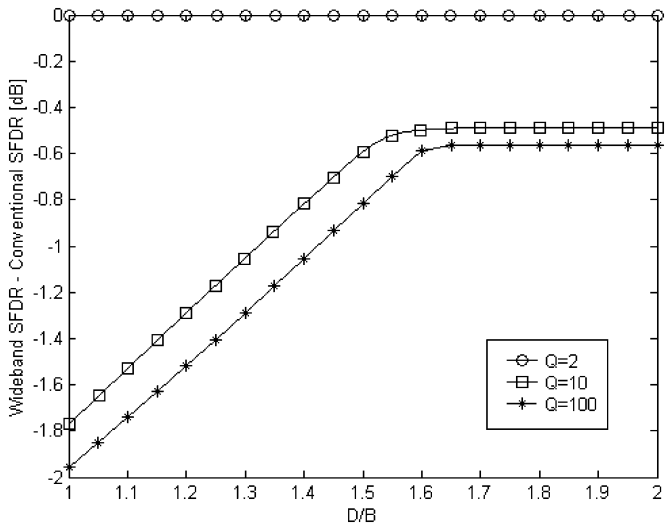

Fig. 5. Comparing the wide-band and conventional SFDR for the memoryless system.

three-toned NL_3. It is important to note that every arrow representing the three-toned NL_3 is repeated. This occurs because, for a fixed value of f_c, the values of f_a and f_b which are different can be interchanged to yield the same f_{NL3}. In our example, arrows 6, 7, and 8 in row $f_{\mathrm{NL3}} = f_2$, which represent the gain desensitization terms, are the same as arrows 1, 4, and 11, respectively. Similarly, arrows 2 and 5 are the same as arrows 9 and 10, all of which correspond to the frequency mix of three different frequencies. Since all three-toned NL_3 are repeated in the arrow diagram, the total number of three-toned NL_3 is simply half of the total number of arrows corresponding to the three-toned NL_3 in the arrow diagram.

For a more general system with Q input tones, the process of maximizing the summation in the denominator of (17) consists of the following steps. We first list all possible NL_3 combinations using the arrow diagram that generate a given f_{NL3}. The next step is to identify the arrows corresponding to the two-toned NL_3 by comparing the direction of the arrows and the row to which they belong. When computing the sum, the weight of one is given to the frequency mix of the two-toned NL_3 whereas the weight of two is given to the rest. This process is repeated by selecting a different f_{NL3} in the frequency band of interest to determine the largest summation value in the denominator of (17).

B. Memoryless System Example

The conventional and wide-band SFDR are compared in a memoryless nonlinear system with constant NF. The input to the nonlinear system consists of two interferers, each with bandwidth B and spacing D as illustrated in Fig. 3. In Fig. 5, the difference between the wide-band and conventional SFDR is plotted as a function of D/B. It is worth noting that this plot is the same regardless of the degree of nonlinearity, since the difference in SFDR is independent of the degree of nonlinearity in a memoryless nonlinear system as can be easily seen by comparing (12) and (17). In Fig. 5, the plots with the circle, square and the star symbols correspond to Q of 2, 10 and 100, respectively. The use of 10 tones seems sufficient to accurately approximate the wide-band SFDR. As the spacing between the two input interferer signal widens, the difference between the wide-band and conventional SFDR gradually reduces from 2 dB (when $D/B = 1$) to approximately 0.6 dB (when D/B is greater than 1.6). Since the difference between the conventional and wide-band SFDR definition is within 2 dB, the conventional SFDR is a reasonably good approximation for memoryless nonlinear systems.

V. Memory Multitone Test

In this section, the equally spaced multitone test is applied to a general memory nonlinear system. In this case, the Volterra kernel is no longer constant but is frequency dependent. The computation of the SFDR given in (16) requires searching for f_{NL3} that minimizes the function in the second bracket. The denominator of this function is computed using a similar enumeration technique as described in the memoryless case, except that the sum of γ_{ab}^2 is weighted by the Volterra kernels. Since knowledge of the Volterra kernel is necessary to determine the SFDR in a general memory nonlinear system, a novel approach for determining the third-order Volterra kernel is first described. The SFDR computation for the low noise amplifier (LNA) is then provided as an example of the general memory nonlinear system.

A. Measuring the Third Order Volterra Kernel

As discussed earlier, the frequency mixes associated with the third-order nonlinear distortion consists of gain expansion/compression, gain desensitization, IM_3 and three-tone frequency mixes. The Volterra kernel for the NL_3 tones generated by the first three frequency mixes can be obtained by applying two input tones; whereas three-tone tests need to be performed to determine the Volterra kernel for the three-tone frequency mix. Note that although the gain desensitization frequency mix is generated by a two-tone test, it is a three-toned NL_3 as stated in Section II.

When determining the Volterra kernels for gain expansion/compression and gain desensitization using the two-tone test, the difficulty is that these two NL_3 tones occur at the same frequency as the input tone frequencies, making differentiating the NL_3 tones from the linear tones impossible. This problem

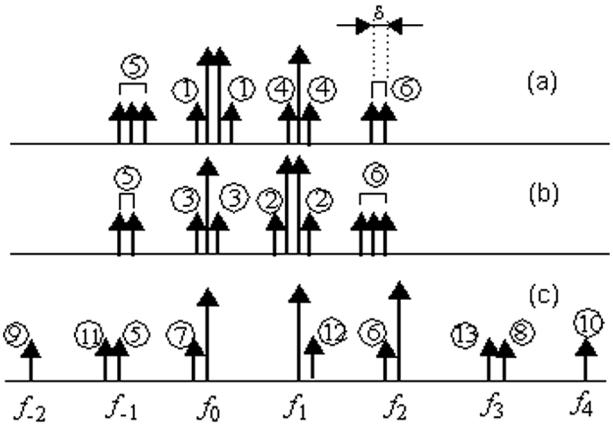

Fig. 6. Measuring the Volterra kernels.

TABLE I
MAPPING THE ARROWS TO THE KERNELS

Gain expansion/ compression	Gain Desensitization	IM_3	NL_3 with 3 frequencies
1. $H_3(f_0,f_0,-f_0)$	3. $H_3(f_0,f_1,-f_1)$	5. $H_3(f_0,f_0,-f_1)$	11. $H_3(f_0,f_1,-f_2)$
2. $H_3(f_1,f_1,-f_1)$	4. $H_3(f_1,f_0,-f_0)$	6. $H_3(f_1,f_1,-f_0)$	12. $H_3(f_0,f_2,-f_1)$
		7. $H_3(f_1,f_1,-f_2)$	13. $H_3(f_1,f_2,-f_0)$
		8. $H_3(f_2,f_2,-f_1)$	
		9. $H_3(f_0,f_0,-f_2)$	
		10. $H_3(f_2,f_2,-f_0)$	

can be overcome by applying three input tones for the two-tone test as shown in Fig. 6(a). Here, the long arrows represent tones at the input frequency and the short arrows are the NL_3 tones generated by the nonlinearity. When applying three tones for a two-tone test at f_0 and f_1, for example, the first two tones are closely spaced at f_0 and $f_0+\delta$ (for δ sufficiently small, e.g., 1 MHz), and the third tone is placed at f_1. The magnitude of the Volterra kernel of the gain expansion/compression and desensitization, i.e., $|H_3(f_0,f_0,-f_0)|$ and $|H_3(f_1,f_0,-f_0)|$, can then be determined by measuring the output power of arrows 1 and 4. The other Volterra kernels for the two-tone frequency mix that cannot be measured from setup in Fig. 6(a) (i.e., $|H_3(f_1,f_1,-f_1)|$ and $|H_3(f_0,f_1,-f_1)|$) can be obtained from the setup in Fig. 6(b). The only difference between the two setups is that the two closely spaced tones are placed at f_1 instead of at f_0. In addition, by performing the experimental setups in Fig. 6(a) and (b), the two Volterra kernels corresponding to the IM_3 kernels, i.e., $|H_3(f_0,f_0,-f_1)|$ and $|H_3(f_1,f_1,-f_0)|$, can also be determined by measuring the output power of arrows 5 and 6.

The Volterra kernels of the three-tone frequency mix is determined by applying a three-tone test. For a three tone test at f_0, f_1 and f_2, for example, three tones are applied at f_0, f_1, and $f_2+\delta$ to prevent the output NL_3 products from overlapping. As shown in Fig. 6(c), the Volterra kernels of $|H_3(f_0,f_1,-f_2)|$, $|H_3(f_0,f_2,-f_1)|$ and $|H_3(f_1,f_2,-f_0)|$ are obtained by measuring the output power of arrows 11, 12 and 13, respectively. In addition, all of the kernels associated with the IM_3 products can also be determined using this three-tone test. The mapping between the output tones and the corresponding Volterra kernel is summarized in Table I.

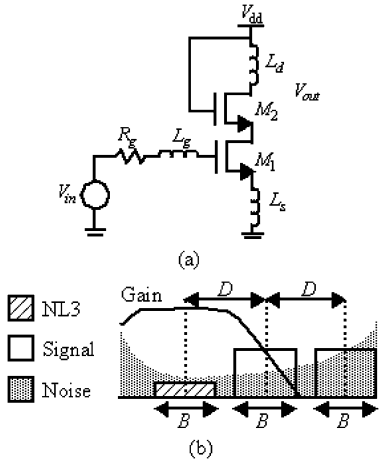

Fig. 7. LNA with reactive degeneration.

Also note that, when estimating the third-order Volterra kernels, the input power is set so that an incremental increase in the input power results in the input referred nonlinear power increasing at approximately three times as fast. In this input power region, the third-order nonlinearity dominates and the higher order nonlinearities can be safely ignored.

When the signal is approximated using Q tones, the number of two-tone tests required to determine the Volterra kernels associated with gain expansion/compression, gain desensitization and the IM_3 terms is the number of combinations of Q tones taken two at a time, i.e., $Q(Q-1)/2$. Similarly, the number of three-tone tests necessary for the Volterra kernel associated with the three-tone frequency mix is the number of combinations of Q tones taken three at a time, i.e., $Q(Q-1)(Q-2)/6$. Although a large number of two-tone and three-tone tests may be required, the tests can be readily automated.

B. Memory System Example

As an example of a memory nonlinear receiving system with frequency dependent NF, a commonly used LNA with inductive degeneration is chosen [13], [14]. Fig. 7(a) shows the circuit schematic of the inductive degeneration LNA, which consists of the cascoded equally-sized MOS transistors (M_1 and M_2) with source degeneration inductor (L_s). The purpose of adding L_s is to provide a 50-Ω input impedance without adding the resistive thermal noise, although lower NF can be achieved by relaxing the 50-Ω constraint. For a given L_s, the LNA resonant frequency can be selected by appropriately choosing inductance values L_g and L_d in Fig. 7(a).

The input to the LNA consists of two interferers, each with bandwidth B and spacing D as illustrated in Fig. 3. As shown in Fig. 7(b), the frequency band of interest is centered at the resonant frequency of the LNA so to achieve maximum linear gain. The 3-dB gain bandwidth of the LNA is denoted as $B_{3\,\mathrm{dB}}$.

In Fig. 8, the wide-band SFDR of the LNA is plotted against $B/B_{3\,\mathrm{dB}}$ for different D/B values. Since the LNA is typically designed so that the LNA gain bandwidth $B_{3\,\mathrm{dB}}$ is greater than the signal bandwidth B, $B/B_{3\,\mathrm{dB}}$ less than one are considered only. To determine the linear and third-order Volterra kernels for the SFDR computation, Cadence SpectreRF was used to simulate an LNA resonating at 2 GHz. The LNA was designed in

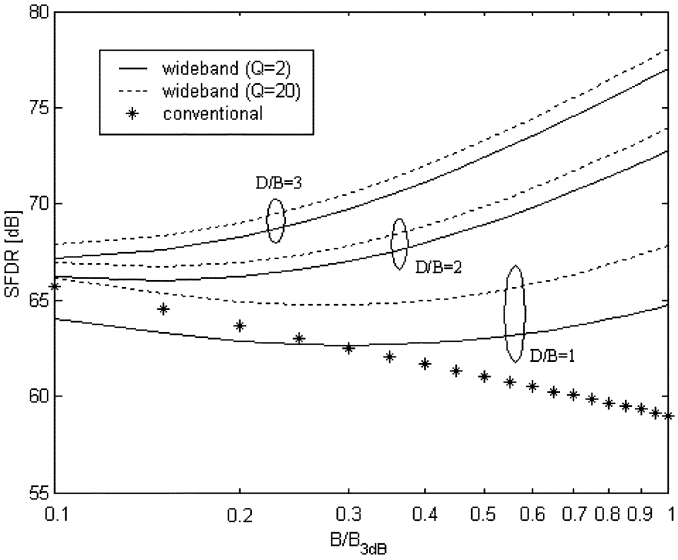

Fig. 8. Comparing SFDR of the LNA using the wide-band and conventional definition.

0.25-μm CMOS technology and dissipates 10 mW. Although not shown, $Q = 20$ tones is sufficient to achieve performance close to infinite tones. In Fig. 8, the difference in the wide-band SFDR between $Q = 2$ (as illustrated by the dash line) and 20 (as illustrated by the solid line) is less than 2 dB. This suggests that the two tone approximation is sufficiently accurate for the wide-band SFDR.

For comparison, the conventional two-tone test is also plotted in Fig. 8. Unlike in the two tone approximation described above, the conventional two-tone test is not well defined when the nonlinear system has memory and/or the NF is not constant in the frequency band of interest. Therefore, the conventional SFDR given in (12) is computed by placing the two tones at the resonant frequency to satisfy the memoryless assumption and by assuming that the NF is the spot NF at the resonant frequency. Unlike the conventional SFDR (as illustrated by the star symbols), the wide-band SFDR first decreases slightly before increasing. A large difference in SFDR is observed between the conventional and wide-band SFDR in memory nonlinear systems. For example when $B = B_{3\,\mathrm{dB}}$, the difference is 5, 12 and 16 dB for $D/B = 1$, 2 and 3, respectively.

VI. Conclusion

The SFDR is commonly used as a measure of dynamic range for the RF and microwave front-end receivers. Since the SFDR is not well defined in wide-band systems, the conventional SFDR is generalized based on a meaningful physical interpretation of the conventional two-tone test. In this definition, multiple input tones are applied to better approximate the input interference signal spectrum. The upper bound of the wide-band SFDR is defined as the minimum signal power at which the maximum NNR is 0 dB and its lower bound is the equivalent noise power obtained using the effective NF. Although a large difference between the conventional and wide-band SFDR is observed for memory nonlinear system, a two-tone test with tones separated in frequency provides reasonably accurate results compared to an infinite-tone test. This suggests that a simple separated two-tone test may be sufficient to quantify a general nonlinear system.

References

[1] W. F. Egan, *Practical RF System Design*. New York: Wiley, 2003.
[2] B. Razavi, *RF Microelectronics*. Englewood Cliffs, N. J.: Prentice Hall, 1997.
[3] W. Namgoong and J. Lerdworatawee, "Noise figure of digital communication receivers-revisited," *IEEE Trans. Circuits Syst. I, Reg. Papers*, vol. 51, no. 7, pp. 1330–1335, Jul. 2004.
[4] G. Crippa, "Evaluation of distortion and intermodulation in nonlinear transmission systems by means of volterra series expansion," *Alta Freq.*, vol. 38, pp. 332–336, May 1969.
[5] M. Schetzen, *The Volterra and Wiener Theories of Nonlinear Systems*. New York: Wiley, 1980.
[6] L. O. Chua and C. Y. Ng, "Frequency domain analysis of nonlinear systems: General theory," *Electron. Circuits Syst.*, vol. 3, pp. 165–185, 1979.
[7] D. D. Weiner and J. F. Spina, *Sinusoidal Analysis and Modeling of Weakly Nonlinear Circuits*. New York: Van Nostrand Reinhold, 1980.
[8] S. A. Maas, *Nonlinear Microwave Circuits*. Norwood, MA: Artech House, 1988.
[9] T. J. Aprille and T. N. Trick, "Steady-state analysis of nonlinear circuits with periodic inputs," *Proc. IEEE*, vol. 60, no. 1, pp. 108–114, Jan. 1972.
[10] J. J. Bussgang, L. Ehrman, and J. W. Graham, "Analysis of nonlinear system with multiple inputs," *Proc. IEEE*, vol. 62, no. 8, pp. 1088–1119, Aug. 1974.
[11] A. Ushida and L. O. Chua, "Frequency domain analysis of nonlinear circuits derived by multitone signals," *IEEE Trans. Circuits Syst.*, vol. CAS-31, pp. 766–777, Sep. 1984.
[12] P. Wambacq and W. Sansen, *Distortion Analysis of Analog Integrated Circuits*. Norwell, MA: Kluwer, 1998.
[13] D. K. Shaeffer and T. H. Lee, "A 1.5-V, 1.5-Hz CMOS low noise amplifier," *IEEE J. Solid-State Circuits*, vol. 32, no. 5, pp. 745–759, May 1997.
[14] A. R. Shahani, D. K. Shaeffer, and T. H. Lee, "A 12-mW wide dynamic range CMOS front-end for a portable GPS receiver," *IEEE J. Solid-State Circuits*, vol. 32, no. 12, pp. 2061–2070, Dec. 1997.

Jongrit Lerdworatawee (S'03) received the B.S. degree in electrical engineering from Tsinghua University, Beijing, China, in 1998, and the M.Eng. degree in electrical engineering from the National University of Singapore, Singapore, in 2000. Since 2000, he has been working toward the Ph.D. degree in the area of analog/radio frequency integrated circuits for telecommunications at University of Southern California, Los Angeles.

His research interests include in the analog/radio frequency and mixed-signal CMOS circuits and system, especially for the front-ends of the ultra-wideBand radio.

Won Namgoong (M'99) received the B.S. degree in electrical engineering and computer science from the University of California at Berkeley, in 1993, and the M.S. and Ph.D. degrees in electrical engineering from Stanford University, Stanford, CA, in 1995 and 1999, respectively.

In 1999, he joined the faculty of the Electrical Engineering Department at the University of Southern California, where he is an Assistant Professor. His current research areas include wireless/wireline communication systems, signal processing systems, RF circuits, and low-power/high-speed circuits.

Dr. Namgoong was the recipient of the National Science Foundation (NSF) CAREER Award in 2002. He currently serves as the Associate Editor of IEEE Transaction on Circuits and Systems—I: Regular Papers.